

AVIRIS SPECTRA OF CALIFORNIA WETLANDS

MICHAEL F. GROSS, College of Marine Studies, University of Delaware, Newark, DE 19716, USA; SUSAN L. USTIN, Department of Botany, University of California, Davis, CA 95616, and Space Sciences Laboratory, University of California, Berkeley, CA 94720; and VYTAUTAS KLEMAS, College of Marine Studies, University of Delaware, Newark, DE 19716.

ABSTRACT

Spectral data gathered by the AVIRIS from wetlands in the Suisun Bay area of California on 13 October 1987 were analyzed. Spectra representing stands of numerous vegetation types (including Sesuvium verrucosum, Scirpus acutus and Scirpus californicus, Xanthium strumarium, Cynodon dactylon, and Distichlis spicata) and soil were isolated. Despite some defects in the data, it was possible to detect vegetation features such as differences in the location of the chlorophyll red absorption maximum. Also, differences in cover type spectra were evident in other spectral regions. It was not possible to determine if the observed features represent noise, variability in canopy architecture, or chemical constituents of leaves.

INTRODUCTION

Gross et al. (1987) analyzed 0.8-1.6 μ m (11 September 1986) AIS-2 data of Suisun Bay, CA, wetlands vegetation and could not identify any narrow-waveband differences between vegetation types, although there were broad-band differences in brightness. The objective of this study is to compare AVIRIS spectra of various wetland vegetation types from the same area to determine how they differ and how these features relate to other land cover types such as soil. Ultimately, we hope to use imaging spectrometry to distinguish vegetation by species (or type) and to measure key chemical constituents, such as chlorophyll, cellulose, lignin, and nitrogen.

DATA ACQUISITION AND ANALYSIS

One flightline of AVIRIS data was acquired over wetland portions of Grizzly Island and Joice Island in Suisun Marsh (Figure 1) on 13 October 1987. The flightline was about 10.5km wide, composed of 614 20m pixels (17% overlap). The area within the flightline is dominated by leveed wetlands that are managed to optimize waterfowl habitat, such that tidal flooding and salinity are controlled, thus causing vegetation distribution and condition to differ between ponds. At the time of data acquisition, lack of rainfall had resulted in senescence of most of the vegetation. In comparison with site conditions at the time of AIS-2 data acquisition, more vegetation was in a senescent condition, and more areas had been recently flooded (starting in September).

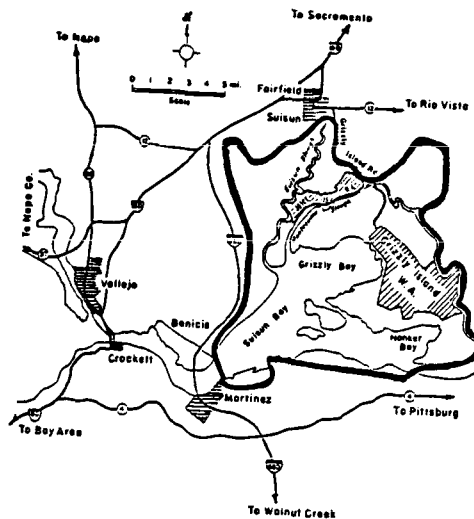


Figure 1. Location of Suisun Marsh
(area within thick solid line)

The data were radiometrically corrected and line drop-outs were removed by averaging at JPL. Data were analyzed using the AVIRIS version of SPAM (Spectral Analysis Manager) software at JPL. Information on land cover types/uses and vegetation distribution was provided by low altitude aircraft photography and high altitude photographs flown at the time of AIS-2 data acquisition. Because the dominant species of vegetation are perennials and often grow in monotypic stands, vegetation distribution does not change substantially over a one year period.

RESULTS

Data quality was generally better than that of AIS-1 and AIS-2 data. Data defects with easily detectable effects included numerous line drop-outs, sudden changes in apparent scene brightness, low signal/noise ratio in Spectrometer D, and fixed pattern noise (particularly evident in Spectrometers A and B). In addition, some horizontal striping was evident (i.e., adjacent rows differed in brightness). Figure 2 shows band 68, or $1.06\mu\text{m}$ (following radiometric rectification). Water and flooded areas appear dark, and dense vegetation appears bright. The fixed pattern noise is evident at the top of the figure as wavy bands oriented diagonally. A sudden change in apparent scene brightness is evident near the bottom of the image.

To derive spectra of various cover types in the image, the mean spectrum of 1×1 to 5×5 pixel samples ($N=4-10$) of distinct vegetation types or soil was computed and considered to represent the spectral response of the cover type. Distinct cover types identified included green Sesuvium verrucosum (purslane), senescing Xanthium strumarium (cocklebur), senescing Cynodon dactylon (bermudagrass), senescing Distichlis spicata (saltgrass), (saltgrass), senescing Scirpus acutus and S. californicus (tules), a senescing mixture of the above vegetation types plus a few others, senescent



Figure 2. Band 68 ($1.06\mu\text{m}$) after radiometric rectification.

mowed tules, senescent unmowed tules and *Typha* (cattails), a flooded area of senescing *Scirpus paludosus* (alkali bulrush), a sparsely vegetated area, two soil areas, and water. These spectra were stored in a library. To better distinguish vegetation spectral features from atmospheric features, all vegetation spectra and one of the soil spectra were multiplied by 50 and then divided by the other soil spectrum using the FUNCTION program (the spectral response of the soil was assumed to approximate that of a flat field).

Spectra were displayed in both normalization modes (area and amplitude). Spectra were compared within five groups of wavebands separated by atmospheric absorption features: $0.45\text{--}0.90\mu\text{m}$, $0.98\text{--}1.11\mu\text{m}$, $1.15\text{--}1.35\mu\text{m}$, $1.49\text{--}1.72\mu\text{m}$, and $1.97\text{--}2.35\mu\text{m}$. Because of the poor signal/noise ratio for Spectrometer D, and possible loss of features for those wavebands resulting from data compression (to achieve a range of 0 to 255 DN), we chose not to analyze the region between 1.97 and $2.35\mu\text{m}$.

As expected, the vegetation spectra were distinct from the soil spectrum by having higher reflectance in the near-infrared relative to the visible region. In addition, there were some other differences between vegetation and soil spectra (for example, vegetation had absorption features at 0.80 , 0.82 , $0.84\mu\text{m}$, a steeper slope between $1.01\mu\text{m}$ and $1.02\mu\text{m}$, a reflectance peak at $1.18\mu\text{m}$ relative to soil, and absorption features at $1.31\mu\text{m}$, $1.51\mu\text{m}$, $1.55\mu\text{m}$, and $1.62\mu\text{m}$).

Green vegetation exhibited an absorption maximum at $0.68\mu\text{m}$, whereas the absorption maximum occurred at $0.67\mu\text{m}$ for senescing vegetation. Comparison of vegetation spectra with each other revealed several other wavelengths at which there was considerable variability in either slope or amplitude of signal. These included $0.76\text{--}0.77\mu\text{m}$, $0.80\text{--}0.84\mu\text{m}$, $1.04\text{--}1.09\mu\text{m}$, $1.29\text{--}1.33\mu\text{m}$, $1.50\text{--}1.52\mu\text{m}$, and $1.57\text{--}1.65\mu\text{m}$. The Xanthium spectrum differed the most from the other spectra. Its notable features included absorption maxima at 0.81 , 1.32 , and $1.51\mu\text{m}$, where other vegetation spectra showed increased reflectance, smaller peaks at 1.29 and $1.56\mu\text{m}$ than the other spectra, and the lack of an absorption feature at $1.62\mu\text{m}$ that was present in other vegetation spectra. The features of various vegetation spectra are evident in Figure 3.

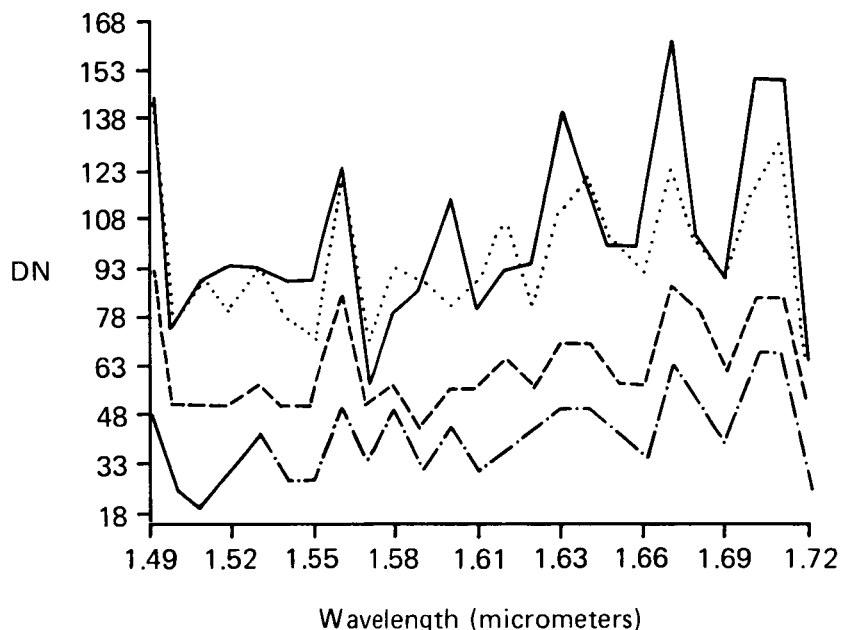


Figure 3. Spectra of four vegetation types, shown between $1.49\text{--}1.72\mu\text{m}$.
 = Cynodon, — = Xanthium, - - - - = Sesuvium, and
 - . - . - . = mixture of wetland vegetation types.

Numerous unsupervised classifications of the image were performed using the CLUSTER algorithm for various portions of the spectral region sampled by the AVIRIS. Results were generally not satisfactory. Most images were "salt and pepper"-like in appearance. Manual and automatic merging of classes did not result in substantial improvement.

Somewhat better results were obtained using MIXTURE, a program that, when used in the "area" mode, assigns pixels to classes based on user-specified spectra (somewhat analogous to a supervised classification). The distribution of cover types assigned by the algorithm corresponded reasonably well to the actual distribution when based solely on spectral characteristics in narrow regions of the spectrum. Tested separately, these included $0.67\text{--}0.72\mu\text{m}$ (Figure 4), $0.74\text{--}0.88\mu\text{m}$, $1.49\text{--}1.72\mu\text{m}$, $1.57\text{--}1.61\mu\text{m}$, and $1.58\text{--}1.64\mu\text{m}$. In Figure 4, the sudden apparent change in scene brightness is evident in columns 2-6, and the fixed pattern noise, in column 6.

Another program that created accurate output was FIND. This program locates all pixels matching a user-defined spectrum within user-supplied allowable deviations in slope and amplitude. The procedure can be repeated for several spectra in one image. In contrast to MIXTURE, FIND works on only one spectrum at a time (i.e., it does not compare all spectral classes with each other and assign pixels to the most likely class). FIND accurately located all Sesuvium and other lush green pixels based on the 0.67-0.72 μ m spectral values. When spectra from several cover types were supplied, reasonably accurate results for this spectral region were obtained, after some manipulation of allowable spectral deviations. Likewise, results were satisfactory when spectra from four spectral regions (0.67-0.68, 0.74-0.76, 1.50-1.52, and 1.56-1.58 μ m) of six cover types were used as input. Other spectral regions were not tested.



Figure 4. Results of MIXTURE analysis, using four spectra (senescent vegetation [column 2], flooded senescing S. paludosus [column 3], green S. verrucosum [column 4], and sparse senescent vegetation [column 5]). Column 1 is the raw image (0.67 μ m), and column 6 is the residual, or pixels whose spectra do not match any of the four spectra. In this case, the residual pixels correspond to water.

DISCUSSION

Our results suggest that, despite considerable noise in the data, the spectral resolution is sufficient to detect differences in the position of chlorophyll absorption maxima.

Also, there may be narrow spectral regions between 0.4-1.72 μ m for which the amplitude and slope of the spectral response of various vegetation types are sufficiently different to enable them to be

distinguished. These include the 0.76-0.77, 0.80-0.84, 1.04-1.09, 1.29-1.33, 1.50-1.52, and 1.57-1.65 μ m areas. Recent attention has been focused on the ability to remotely sense canopy chemical constituents based on their absorption features. Peterson et al. (1988), Norris et al. (1976), and Burdick et al. (1981) report significant correlations between the concentration of chemical constituents and reflectance at various wavelengths, principally between 1.55-1.75 μ m and between 1.95-2.35 μ m. The specific wavelengths useful for detecting these constituents seem to vary from study to study and to depend on whether the raw spectra, first derivative, second derivative, or some other transformation is being used. Our results indicating the presence of some species-dependent differences in spectra may reflect variations in canopy architecture (including the influence of soil), the concentration of major chemical constituents, or some combination of these factors. We did not have the resources to chemically analyze vegetation samples, so we can only speculate about the significance of these spectral features. Because of the data quality problems mentioned above and our division of vegetation spectra by a soil spectrum, it is likely that some apparent spectral features were not real. However, we tried to minimize this possibility by sampling, for each spectrum, a large number of pixels scattered throughout the image.

Future research efforts should be directed towards obtaining spectral measurements of the vegetation on the ground, and measuring the concentration of chemical constituents in the vegetation to understand the features in the spectra sensed by the AVIRIS. Initial studies could focus on determining what constituents influence reflectance at 0.76-0.77 μ m, 0.80-0.84 μ m, 1.04-1.09 μ m, 1.29-1.33 μ m, 1.50-1.52 μ m, and 1.57-1.65 μ m.

ACKNOWLEDGEMENTS

This research was supported by the NASA Earth Science and Applications Division Land Processes Program under Grant No. NAGW-950, and the Universities of Delaware and California. The authors are indebted to Lorena Hobart for secretarial expertise, and the staff at JPL for processing the raw data and allowing us to use their image analysis facility (special thanks go to Lisa Barge for help with SPAM).

LITERATURE CITED

- Burdick, D., F. E. Barton, II, and B. D. Nelson. 1981. Prediction of bermudagrass composition and digestibility with a near-infrared multiple filter spectrophotometer. Agron. J. 73:399-403.
- Gross, M. F., S. L. Ustin, and V. Klemas. 1987. AIS-2 spectra of California wetland vegetation, pp. 83-90 in Proc. Third AIS Data Anal. Workshop, JPL Publ. 87-30, Jet Propulsion Lab, Pasadena, CA.
- Norris, K. H., R. F. Barnes, J. E. Moore, and J. S. Shenk. 1976. Predicting forage quality by infrared reflectance spectroscopy. J. Animal Sci., 43:889-897.
- Peterson, D. L., J. D. Aber, P. A. Matson, D. H. Card, N. Swanberg, C. Wessman, and M. Spanner. 1988. Remote sensing of forest canopy and leaf biochemical contents. Remote Sens. Environ., 24:85-108.